Formation of One-dimensional Image by Pulsed Light Diffraction on Running Sound Wave

Victor Petrov[1] **and Roman Kijan**[2]

[1]St.-Petersburg Politechnical University, St.-Petersburg, Russia
[2]Laser Zentrum Hannover e.V., Hannover, Germany

Abstract— The advanced systems for formation of a TV image on a projection screen is an acoustooptic system that relies on the principle of exposure of the entire TV 1D image by one laser pulse and further deflection of 1D images across the frame. The case of a diffracted field for wide-band anisotropic light diffraction by a slow shear elastic wave near the optical axis of an acoustooptic modulator made from a crystal of paratellurite TeO_2 was considered. We rely on the solution for the diffracted field and consider the problem of formation of the image of an amplitude-modulated 1D image that fills the acoustooptic modulator aperture on the projection screen. As a light source, a copper-vapor laser with wavelength $\lambda_0 = 0.5106\,\mu\mathrm{m}$ and generation pulse duration $\tau_0 = 10\,\mathrm{ns}$ was used.

1. THE CASE OF A LOW EFFICIENCY OF ACOUSTOOPTIC INTERACTION FOR CONVERGING LIGHT BEAM

Let us consider the system for formation of a 1D image (Figure 1) that includes an acoustooptic modulator (AOM), input cylindrical lens L_1, and an objective consisting of lenses L_2 and L_3. The $X'0Z'$ and $Y'0Z'$ planes of the system are chosen so that in one of them ($X'0Z'$) light diffraction in the AOM and formation of the 1D image on the screen Sc occur, and in the other plane ($Y'OZ'$) formation of the spatial distribution of the 1D image and its deflection in the screen plane takes place. The medium for the acoustooptic interaction is a TeO_2 crystal.

Our consideration refers to the interaction geometry which is employed in a real device (Figure 2) and which corresponds to the case of wide-band anisotropic light diffraction by a slow shear elastic wave [1, 2].

We assume that an ultrasonic wave with the polarization vector directed along the [110] axis coinciding with the Y' axis propagates along the $[\bar{1}\ 10]$ direction of the crystal coinciding with the X' axis of the optical system. The wave vector of the light wave **k** makes angle θ with its projection on the (110) plane, and the projection of this vector on the (110) plane is at angle α to the Z' axis.

Angles α and θ are assumed to be small, and we have

$$\begin{gathered} k'_x, k'_y \ll k; k'_x = k_x = -k\sin\theta \approx -k\theta; \\ k'_y = k\cos\theta\sin\alpha \approx -k\alpha \end{gathered} \tag{1}$$

where $k = 2\pi/\lambda_0$ is the amplitude of the wave vector of the light wave for a free space.

Then, following by a formalism, developed in [2], using the same notations, and by assuming that the light pulse shape corresponds to the Gaussian distribution law and also that the light source coherence time $\tau_{\mathrm{coh}} = l_{\mathrm{coh}}/c$ (l_{coh} is the longitudinal coherence length) is much shorter than the radiation pulse duration (this is fulfilled, for example, for the copper-vapor laser), we get the time-average distribution of light intensity in the 1D image on the screen

$$\begin{aligned} I\left(x'_1, y'_1\right) &= \frac{1}{T}\int_{-\infty}^{+\infty} \exp\left\{-\frac{t^2}{\tau_0^2}4\ln 2\right\} I_1\left(x'_1, y', t_1\right) dt \\ &= \Gamma_0\left\{D_0 + m_0\exp\left\{-\frac{\pi f_0\tau_0}{2\sqrt{\ln 2}}\right\}^2\sqrt{D_1^2+D_2^2}\sin\left(\frac{2\pi f_0}{\nu}x'+\Delta_1\right)\right. \\ &\quad \left. +\frac{m_0}{2}\exp\left\{-\frac{\pi f_0\tau_0}{2\sqrt{\ln 2}}\right\}^2\sqrt{D_3^2+D_4^2}\sin\left(\frac{4\pi f_0}{\nu}x'+\Delta_2\right)\right. \end{aligned} \tag{2}$$

where T is the period over which time integration is performed; and τ_0 is the light pulse duration at the 0.5 light intensity level. The first term in Expression (2) defines the constant component

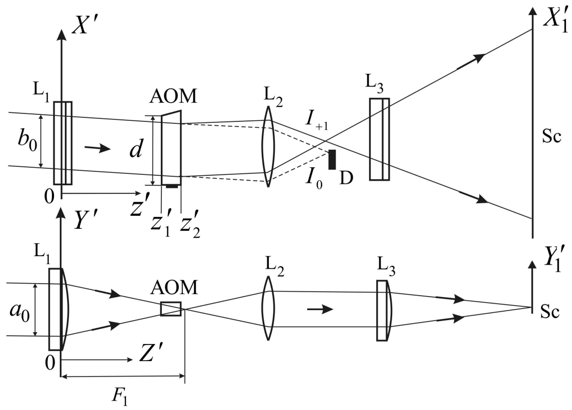

Figure 1: Optical scheme of the system for formation of a 1D image in two mutually perpendicular planes: AOM — acoustooptic modulator; L_1 — input cylindrical lens; L_2, L_3 — lenses of the objective; Sc — screen; D — diaphragm; I_0, I_{+1} — intensities of the incident and diffracted light beams; a_0, b_0 — light beam sizes along two coordinates; F_1 — focal distance of L_1; d — acoustooptic modulator size along the X' axis.

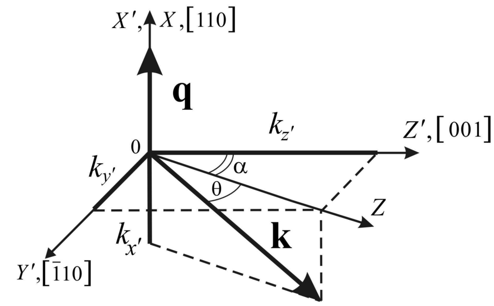

Figure 2: Geometry of acoustooptic interaction: $\mathbf{k}$, $\mathbf{k}_s$ — wave vectors of light and sound waves; $k_{x'}$, $k_{y'}$, $k_{z'}$ — projections of vector $\mathbf{k}$ on the coordinate axes; θ — angle between wave vector $\mathbf{k}$ and its projection on the (110) plane; α — angle between the Z' axis and projection of vector $\mathbf{k}$ on the (110) plane.

in the signal of the image, the second term gives modulation with the input signal frequency, and the third term describes nonlinear distortions in the image at a doubled signal frequency. Coefficient Γ_0 characterizes changes in the average light intensity in the 1D image on the screen due to transformation of the light beam sizes.

2. MODULATION-TRANSFER FUNCTION OF THE SYSTEM

The Expression (2) corresponds to the case of a low diffraction efficiency. Let us use this expression to find the modulation-transfer function (MTF) of the system. To this end, we consider the cross section of this distribution by the plane $y = y_0$ for which $I(y_0) = I_{\max}$. We define the contrast transfer function versus modulation frequency f_0 as

$$M\left(f_0\right) = I_{\max}\left(f_0\right) - I_{\min}\left(f_0\right) / I_{\max}\left(f_0\right) + I_{\min}\left(f_0\right) \tag{3}$$

Function (3) was calculated for different light pulse durations τ_0 and cones of angles of light incidence on the sound beam $2\tilde{\alpha}$ which corresponded to the choice of different focal distances F_1 for different central frequencies of ultrasound f and Bragg angles $\theta_0^{(0)}$, $\theta_0^{(1)}$ corresponding to these frequencies, and also for different acoustooptic interaction lengths L. The medium for the acoustooptic interaction was the TeO_2 crystal. The light radiation wavelength in the calculations was taken to be 510.6 nm, which corresponded to the green line of the copper-vapor laser, and the ultrasonic wave modulation depth was $m_0 = 1$.

Calculations showed that $M(f_0)$ was nearly independent of the cone of the angles of incidence $2\tilde{\alpha}$ in the plane orthogonal to the scattering plane. Its shape was mainly determined by the choice of the carrier frequency of ultrasound f, ultrasonic beam with L, and light pulse duration τ_0. Figure 3 shows calculated MTF families for different parameters. It can be seen that as the light pulse duration becomes smaller, the decrease in the MTF slows down. As ultrasonic beam sizes reduce (interaction length L, Figure 3(b)) the MTF decrease becomes slower which can be explained by an increase in the spatial-frequency region of acoustooptic interaction due to broadening of the directional diagram of the elastic wave emitter. In all the cases a decrease in length L leads to an increase in the contrast in the image transfer.

Figure 4 shows the dependence of coefficient N on modulation frequency f_0 plotted for the same functions $I(f_0)$ as in Figure 3(a).

$$N\left(f_0\right) = \ln\left\{I_{\max}\left(f_0\right) / I_{\min}\left(f_0\right)\right\} \tag{4}$$

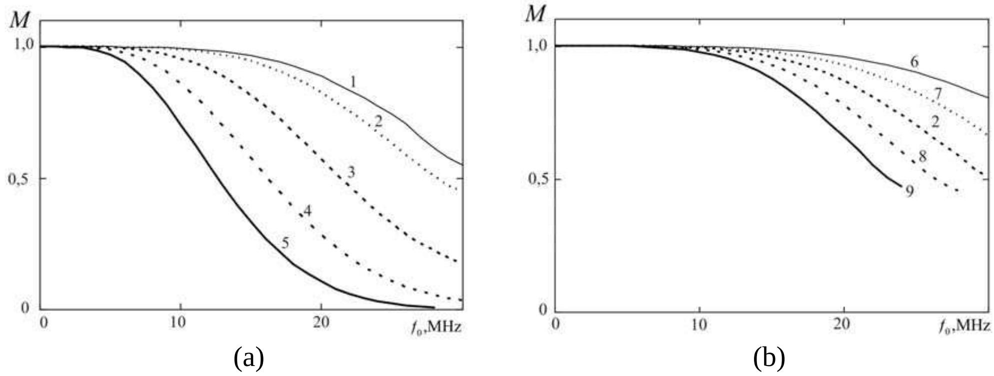

Figure 3: (a)MTF of the system as a function of light pulse duration τ_0, (b) interaction length L, basic set of parameters: $f = 80\,\text{MHz}$; $L = 4\,\text{mm}$; $\tau_0 = 10$ ns (curves 2); τ_0, ns: 5 (1), 10 (2), 20 (3), 30 (4), 40 (5); L, mm: 2 (6); 3 (7), 4 (2), 5 (8), 6 (9).

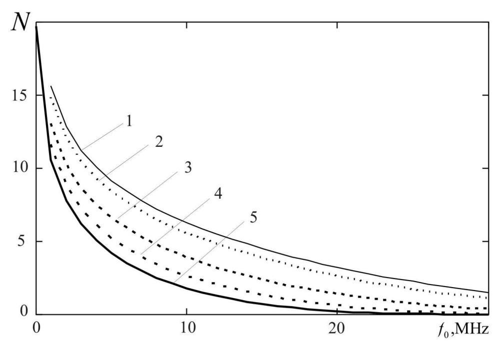

Figure 4: Logarithmic contrast transfer function for different pulse durations τ_0, ns: 5 (1), 10 (2), 20 (3), 30 (4), 40 (5).

The number of tone levels the eye can perceive is taken to be

$$N\left(f_0\right) = \frac{1}{\sigma} \ln \left\{I_{\max}/I_{\min}\right\} \tag{5}$$

where σ is the threshold contrast; $\sigma = 0.02$–0.05. The dependences in Figure 4 can be useful for estimation of the number of tone levels (gray levels) and highest frequency of the image the eye can perceive. If we assume that the highest MTF frequency is the frequency $f_0 = f_h$ at which $N(f_h) = \sigma$ and solve the relevant equations, we obtain that at $\tau_0 = 40\,\text{ns}$ the highest frequency is $f_h \cong 25\,\text{MHz}$, at $\tau_0 = 30\,\text{ns}$ $f_h \cong 31\,\text{MHz}$, and at $\tau_0 = 20\,\text{ns}$ $f_h \cong 50\,\text{MHz}$.

3. RESULTS AND CONCLUSIONS

In the approximation of a low diffraction efficiency, a two-dimensional field distribution in the (+1)st diffraction order in the focal plane of the input cylindrical lens and a time-average distribution of intensity of light from a pulsed coherent source in the image plane have been calculated. Calculations of the modulation-transfer function of the acoustooptic system for the 1D image formation including a pulsed copper-vapor laser and AOM from a paratellurite crystal (TeO_2) for different light pulse durations, carrier frequencies of ultrasound, acoustooptic interaction lengths, and also angles of light incidence on the AOM in the plane orthogonal to the scattering plane have been carried out.

Numerical calculations have shown that an increase in the light pulse duration leads to a decrease in the contrast in transfer of amplitude-modulated signals at high frequencies. An increase in the contrast at high frequencies results from a decrease in the piezotransducer width and decrease in the carrier frequency of ultrasound. It approaches the frequency of two-phonon interaction.

Requirements to the choice of the focal distance of the input cylindrical lens and cone of angles of light incidence on the AOM in the plane orthogonal to the plane of diffraction at which no noticeable decrease in the average intensity of diffracted light occurs have been formulated.

REFERENCES

1. Petrov, V., "Digital holography for bulk image acoustooptical reconstruction," *Digital Holography and Three-dimensional Displays: Principles and Applications*, 73–99, 430, by Ting-Chung Poon, Ed., Springer, 2006.
2. Korikov, C., Y. Mokrushin, and R. Kiyan, "Transmitting of a full-TV image by a pulsed one-dimensional serial optical frames: A non-linear approach," *Internet of Things, Smart Spaces, and Next Generation Network and Systems*, 662–675, 716, S. Balandin, et al., Eds., Springer, 2014.